Effect of germination on the functional and moisture sorption properties of high pressure processed foxtail millet grain flour

Article

Accepted Version

It is advisable to refer to the publisher's version if you intend to cite from the work. See Guidance on citing.

www.reading.ac.uk/centaur

CentAUR

Central Archive at the University of Reading

Reading's research outputs online

1 **Effect of germination on the functional and moisture sorption properties of high**

2 **pressure processed foxtail millet grain flour**

3 Nitya Sharma[a]*, S.K. Goyal[a], Tanweer Alam[b], Sana Fatma[c], Keshavan Niranjan[d]

4 [a]Department of Farm Engineering, Institute of Agricultural Sciences, Banaras Hindu

5 University, Varanasi (India)

6 [b]Indian Institute of Packaging, New Delhi (India)

7 [c]Centre of Food Science and Technology, Banaras Hindu University, Varanasi (India)

8 [d]Department of Food and Nutritional Sciences, University of Reading, Reading (UK)

9 [*] Corresponding author email ID: nitya.sharma64@gmail.com

10 **Abstract**   Foxtail millet is one of the commonly cultivated, nutritionally competitive

11 source of protein, fibre, phytochemicals and other micronutrients, as compared to major

12 cereals like wheat and rice. Considering the potential of these grains, the high pressure

13 processed flours of germinated (GFMF) and non-germinated foxtail millet (NGFMF) grains

14 were studied for its functional, moisture sorption and thermodynamic properties. Germination

15 and high pressure processing of foxtail millet grains significantly improved the functional

16 properties of the flour. Apart from this, the moisture sorption isotherms of both the flours

17 were determined at 10, 25 and 40 $^{\circ}$C and the sorption data was fitted to Guggenheim-

18 Anderson-De Boer (GAB) sorption model. The monolayer moisture content for NGFMF and

19 GFMF ranged between 3.235 - 2.364 g g^{-1} and 2.987 – 2.063 g g^{-1}, respectively. The isosteric

20 heat of sorption ranged between -76.35 kJ mol^{-1} to -38.23 kJ mol^{-1} for NGFMF and 172.55 kJ

21 mol^{-1} to -34.02 kJ mol^{-1} for GFMF at a moisture range of 0 to 36%, whereas, the integral

22 entropy of sorption for NGFMF ranged between -0.404 to -0.120 kJ mol^{-1} K^{-1} and for GFMF

23 between -0.667 to -0.383 kJ mol^{-1} K^{-1}. Along with the validation of the compensation theory,

24 the values of spreading pressures lied in the range of 0 – 0.078 J m^{-2} for NGFMF and 0 –

25 0.124 J m^{-2} for GFMF, while, the glass transition temperatures ranged between 82.25 to 28.67

26 $^{\circ}$C for NGFMF and from 51.11 to 11.83 $^{\circ}$C for GFMF at all three temperatures.

27 **Keywords**   Foxtail millet flour, germination, high pressure processing, functional

28 properties, moisture sorption isotherms, thermodynamic properties

29

Introduction

Water sorption characteristics are necessary for predicting the shelf life and determining the moisture content and critical activity for acceptability of products that deteriorate, mainly due to moisture gain, and also for drying, packaging and storage (Katz and Labuza 1981). A food moisture sorption isotherm describes the relationship between the moisture uptake in food and the relative humidity of the air with which the food is in equilibrium at a constant temperature (Lagoudaki et al. 1993). Thermodynamics has been reported as an approach to understand the properties of water and calculate the energy requirements of heat and mass transfer in biological systems (Rizvi and Benado 1983; Fasina et al. 1997; Fasina et al. 1999). Properties such as isosteric heat of sorption, net integral enthalpy and entropy and spreading pressures are important for understanding the energy requirement during dehydration, the food microstructure, physical phenomena on the food surfaces and sorption kinetic parameters (Rizvi and Benado 1983). Also, the glass transition temperature is an important physical parameter, which serves to explain the physical and chemical behaviour of food systems (Bell and Labuza 2000), and it is defined as the temperature at which the material changes from the glassy to the rubbery state for a given heating rate.

Foxtail millet (*Setaria italica* (L.) P. Beauv.) is the sixth highest yielding grain amongst all the millet varieties and has been identified as a major millet in terms of worldwide production (Sharma et al. 2017). Foxtail millet ranks second in the total world millet production of around 29 million tonnes (in 2015-16 season). It originates in the Yellow River Basin country, which makes China a leading foxtail millet producer holding 80% of world production, followed by India with 10% of world production (Zhang et al. 2017). Foxtail millet is one of the oldest cultivated cereal grains belonging to the *Setaria* genus, of *Poaceae* family and subfamily *Panicoideae*. Sharma et al. (2017) have discussed the versatility of foxtail millet as a food source and its potential to address food and nutrition security. These authors have reviewed the effects of various processing techniques on the properties of foxtail millet grains.

It has been recognised that non-thermal processing techniques like high hydrostatic pressures (HHP), can potentially inactivate anti-nutritional factors like phytate and tannin content in cereal grains and preserve their constituents and quality (Estrada-Girón et al. 2005; Yu et al. 2015; Zhang et al. 2017). In addition to high pressure processing, germination, is one of the traditional approaches used to supplement the bio-accessibility of nutrients in plant-based

62 diets. The process of germination in cereal grains results in an increase in enzymatic activity,

63 soluble protein content and break down of starch into simple sugars, resulting in the

64 formation of typical colours and flavours (Barreiro et al. 2003). Moisture sorption properties

65 have also been studied for various cereals and its products like various cereal grains and

66 legumes (Al-Mahasneh et al. 2014), milk-foxtail millet powder (Simha et al. 2016), two

67 millet grain varieties (Aviara et al. 2016), tef (*Eragrostis tef* (Zucc.) Trotter) grain flour

68 (Abebe and Ronda 2015), bulgar (Erbaş et al. 2015), Greek durum wheat semolina (Pollatos

69 et al. 2013), RTE breakfast cereal formulation (Sandoval et al. 2009), oat and rice flour (Brett

70 et al. 2009), maize meal and millet flours (Ikhu-Ornoregbe and Chen 2005). In general, very

71 limited moisture sorption data is available for germinated cereals, especially for high pressure

72 processed and germinated millet grains. This study was therefore conducted to assess the

73 effect of germination on the functional, moisture sorption and thermodynamic properties of

74 high pressure processed foxtail millet grain flour.

75 **Materials and methods**

76 **Sample collection**

77 Foxtail millet (*Setaria italica* L.) grains were procured from authorized grain centres. All

78 procured grains were a month old since harvesting and were tested for viability using

79 tetrazolium chloride test (Lakon 1949). The moisture content of the native grains was found

80 to be 8.41±0.45%, following which the grains were stored in polythene bags at 4 °C until

81 further use. The chemicals used for analysis were procured from Sigma-Aldrich Chemical

82 Co., (St. Louis, Mo, USA).

83 **Germination of foxtail millet grains**

84 The foxtail millet grains were washed using 1.5% formaldehyde solution to prevent any

85 contamination. To remove the traces formaldehyde, the grains were then washed thoroughly

86 with distilled water and tested for any residues using the ferric chloride method described by

87 VICH Steering Committee (2002). Prior to germination, the foxtail millet grains were first

88 soaked in deionised water for 15h and then were subjected to germination in a controlled-

89 environment growth cabinet. The temperature was maintained at 25±2 °C and the relative

90 humidity was controlled at 50%; these conditions were based on the work reported by

91 Sharma et al. (2015). Following the method described by Elkhalifa and Bernhardt (2010), the

92 activities of alpha amylase and protease were monitored at regular intervals of 12 hours, and

93   the germination period of 72h represented the time taken for their activities to reach a

94   maximum value., as. The maximum alpha amylase and protease activity was found to be

95   attained after 72h (Fig. 1). The germinated foxtail millet grains were dried to a final moisture

96   content of 7 – 8%, packed and stored in air-tight containers at 4 °C until further analysis.

97   Non-germinated foxtail millet grains were used as a control.

High pressure soaking

99   Both germinated and non-germinated foxtail millet grains (25g each) were subjected to high

100   hydrostatic pressures in a temperature-controlled pressure vessel system (vessel dimensions:

101   37mm diameter and 246mm length, Food LAB 900, Stansted Fluid Power Ltd., Stansted,

102   UK). A blend of castor oil and ethanol in a ratio of 80:20 v/v was used as a medium to

103   transmit pressure to the packed samples in the pressure vessel chamber. The foxtail millet

104   grains were treated at a pressure of 400 MPa for 60 mins at a temperature of 60 °C. For this,

105   25g foxtail millet grain samples were suspended in 150ml of deionised water and sealed with

106   virtually no headspace polyethylene pouches of dimensions 3cm × 20cm by employing

107   Cryovac[TM]. All the experiments were triplicated.

108   After high-pressure processing under specified conditions of pressure and temperature for a

109   stipulated time, the water was completely drained from the pouches and the water occluding

110   to the grains separated, was then blotted using a tissue paper. The processed grains were then

111   subjected to freeze drying and were finally milled into fine flour passing through sieves of

112   mesh sizes ranging between 100 and 200µm, using vibratory sieve shaker (Fritsch Analysette

113   3, Germany). The resulting flour was packed and stored in air-tight containers at 4 °C until

114   further analysis.

Determination of functional properties

116   The bulk density, porosity and flowability of the optimized foxtail millet flour, as the angle of

117   repose (as a static measure for flowability), were determined by the method of Sjollema

118   (1963). The occluded air content was determined by the methods used by Jha et al. (2002).

119   The wettability was determined by the method given by Muers and House (1962). The

120   dispersibility of the optimized baby food was determined by the method described by the

121   American Dry Milk Institute (ADMI 1965). The insolubility index was determined by the

122   modified ADMI method described by Jha et al. (2002). The water, oil absorption capacity

123   and swelling capacity of the product were determined by the method described by Sodipo and

4

124   Fashakin (2011). The emulsion activity, emulsion stability, foaming capacity and foaming

125   stability were determined using the methods described by Elkhalifa and Benhardt (2010).

126   Finally, the gelatinization temperatures were determined using Differential Scanning

127   Calorimetry, where a suspension of the resulting flour in deionised water was prepared in a

128   ratio of 1:3; equilibrated for 15-18 h at ambient temperature; and presented to the differential

129   scanning calorimeter, equipped with a built-in software (Model Q 2000a TA Instruments,

130   New Castle, U.S.A.). A 10-12 mg suspension sample was weighed precisely in an aluminium

131   sample pan and hermetically sealed. A similar empty pan was used as a reference for the

132   analysis. A temperature range of 10 to 140 $^{\circ}$C was used for scanning the sample in the pan at

133   a heating rate of 10 $^{\circ}$C min^{-1}. The resulting thermogram gave the values of onset (T_o), peak

134   (T_p) and conclusion temperatures (T_c) in $^{\circ}$C.

Sorption studies

136   Gravimetric method described by Lang et al. (1981), was used to determine the sorption

137   isotherms for processed foxtail millet flour. The saturated salt solutions of eight reagent-grade

138   salts, namely, lithium chloride, magnesium chloride, potassium carbonate, magnesium nitrate,

139   sodium chloride, potassium chloride, potassium nitrate, and potassium sulfate, were chosen as

140   mentioned by Greenspan (1977) to cover the water activity range from 0.11 to 0.97. It is

141   important to note that the water activity values for these salts can show slight variations at

142   different temperatures. Therefore, different water activity values of these salts at temperatures

143   10, 25 and 40 $^{\circ}$C were used in this study. These saturated solutions were placed in air tight,

144   wide mouth glass jars. Approximately 1 g of sample was weighed into a glass beaker placed

145   on glass bead support inside the glass jar. The glass beakers were equilibrated for three days

146   with the humid atmosphere before placing the sample. Then the moisture sorption

147   characteristics were studied at 10, 25 and 40 $^{\circ}$C ($\pm$ 2 $^{\circ}$C) by placing the sample containing

148   glass jars in incubators for equilibration. These conditions were chosen in this study, as they

149   represent the possible storage conditions for cereals like rice (Ondier et al. 2012) The samples

150   in bottles were weighed at a regular interval of 3 days till a constant weight was attained.

151   Equilibrium was considered to have accomplished when the weight difference between two

152   successive weighing was less than 1 mg. Experiment was conducted in triplicates for all the

153   samples at each relative humidity and temperature conditions. After the equilibrium has been

154   attained, the moisture content of the samples was determined and was expressed in gram per

155   litre (g/L). The average standard deviation between the replicates was calculated to be less

156 than 1% of the mean of the three values. These average values of equilibrium moisture
157 content were then plotted against relative humidities or water activities to obtain moisture
158 sorption isotherms.

159 *Sorption model*

160 Various approaches have been used to describe sorption isotherms of foods. Amongst which,
161 Guggenheim-Anderson-De Boer (GAB) (Pérez-Alonso et al. 2006) is mostly used to study
162 the correlation between the equilibrium moisture content (M) and water activity (a_w) for
163 various foods. The following linearized form of GAB model were used for evaluating the
164 best fitted values of model constants using linear regression:

165 GAB

166 $$W = W_o \frac{Gka_w}{(1-ka_w)(1-ka_w+Gka_w)}$$ (1)

167

168 The GAB model could be rearranged into a second-degree polynomial equation as given
169 below:

170 $$\frac{a_w}{W} = aa_w^2 + ba_w + c$$ (2)

171 where, a, b and c are model constants and significantly depend on type of regression analysis.
172 A nonlinear regression analysis of a_w/W v/s a_w yields a polynomial equation of the second
173 order. The coefficients a, b and c were thus obtained from this polynomial equation and then
174 substituted to obtain GAB constants W_o, G and k. W_o is the moisture content corresponding to
175 saturation of all primary adsorption sites by one water molecule, G is the Guggenheim
176 constant and k is the factor correcting for properties of multilayer molecule with respect to
177 the bulk liquid.

178 *Thermodynamic properties*

179 The integral enthalpy, also known as, net isosteric heat of sorption was determined using
180 Clausius-Clapeyron equation (Rizvi 1986; Bell and Labuza 2000):

181 $$\frac{\partial(lna_w)}{\partial(\frac{1}{T})} = \frac{Q_{st}}{R}$$ (3)

182   where, T is the absolute temperature (K), Q_{st} is the net isosteric heat of sorption (kJ mol^{-1})

183   and R is the universal gas constant (8.314 × 10^{-3} kJ mol^{-1} K^{-1}).

184   The calculation procedure assumed that net heat of sorption was independent of temperature

185   change. The slope of the plot of ln (a_w) versus $1/T$ at constant moisture content gave the net

186   isosteric heat of sorption (Eq. 3). Adding the latent heat of vaporization of pure water at 10,

187   25 and 40 °C to the net isosteric heat of sorption (Q_{st}), gave the values of isosteric heat of

188   sorption. A cubic spline interpolation was used to determine a_w values at various

189   temperatures for a given moisture content (M).

190   Substituting free Gibbs energy in the Gibbs- Helmholtz equation (McMinn and Magee 2003;

191   Kaya and Kahyaoglu 2005), the differential entropy was calculated using the following

192   equation:

193    $$-\ln(a_w) = \frac{-(Q_{st}+\lambda)}{RT} - \frac{\Delta S}{R} \tag{4}$$

194   where, λ is the latent heat of vaporization of pure water (44.045 kJ mol^{-1} at 25 °C), and ΔS is

195   the integral entropy of sorption (kJ mol^{-1} K^{-1}). The maximum storage stability point is when

196   the water activity and temperature gives the minimum value of integral entropy (Alpizar-

197   Reyes et al. 2017).

198   From the intercept of the plot of ln (a_w) versus $1/T$ at specified moisture levels of eq. (4), the

199   integral entropy was evaluated.

200   *Isokinetic theory*

201   A linear relationship between the isosteric heat of sorption (differential enthalpy) and

202   differential entropy established the enthalpy- entropy theory (McMinn and Magee et al.

203   2003; Arslan and Togrul 2006):

204    $$Q_{st} = T_\beta \Delta S_d + \alpha \tag{5}$$

205   where, Q_{st} is the isosteric heat of sorption (kJ mol^{-1}), T_β is the isokinetic temperature (K), and

206   α is the constant or Gibb's free energy (kJ mol^{-1}).

207   The isokinetic temperature (T_β) is a characteristic property of the material surface (Aguerre

208   et al. 1986), and it represents the slope of the enthalpy- entropy linear relationship (Eq. 5).

209 Linear regression of Q_{st} with ΔS_d evaluated T_β. A statistical test proposed by Krug et al.

210 (1976) verified the enthalpy- entropy compensation theory by defining the harmonic mean

211 temperature (T_{hm}) as:

212 $$T_{hm} = \frac{n}{\sum_1^n (\frac{1}{T})}$$ (6)

213 where, T_{hm} is the harmonic mean temperature (K), and n is the number of temperature levels.

214 Linear enthalpy- entropy compensation theory applies only when $T_\beta \neq T_{hm}$; the process is

215 enthalpy driven if $T_\beta > T_{hm}$ and entropy driven if $T_\beta < T_{hm}$ (Leffler and Grunwald 1963). Eq.

216 (6) shows that T_{hm} is a function of temperature levels selected for the experiment and is

217 independent of the material considered. Analyses were conducted with $\alpha = 0$ to evaluate the

218 effect of temperature on the sorption behaviour by introducing a temperature correction factor

219 (Aguerre et al. 1986) as:

220 $$-\ln(a_w) = \frac{Q_{st}}{R(\frac{1}{T} - \frac{1}{T_\beta})^{-1}}$$ (7)

221 *Spreading pressures*

222 Spreading pressure was evaluated based on the analytical procedure described by Iglesias et

223 al. (1976) and Fasina et al. (1999). Spreading pressure is given by the following equation:

224 $$\pi = \frac{KT}{A_m} \int_0^{a_w} \frac{x}{x_m a_w}$$ (8)

225 where, π is the spreading pressure (J m^{-2}), K is the Boltzman constant (1.380×10^{-23} J K^{-1})

226 and A_m is the surface area of a water molecule (1.06×10^{-19} m^2).

227 This integral becomes indeterminate at $a_w = 0.0$. Therefore, spreading pressure was evaluated

228 by dividing the total limit (0.0 to a_w) into a very small interval of 0.0 to 0.05 and the

229 remaining 0.05 to a_w. The integral in the first infinitesimal a_w range (0.0 to 0.05) was

230 evaluated assuming a linear relationship (Henry's law) between m and a_w with usual notations

231 (Fasina et al. 1999) as:

232 $$\pi = \frac{KTx}{A_m x_m}$$ (9)

233   The integral in the second a_w range (0.05 to a_w) was evaluated after fitting isotherm data (m,

234   a_w) to the GAB model equation and the spreading pressure was obtained by integrating the

235   equation in the second interval of 0.05 to a_w (Iglesias et al. 1976):

236   $$\pi = \frac{KT}{A_m} ln \left[\frac{1+Cka_w-ka_w}{1-ka_w} \right]_{0.05}^{a_w}$$ (10)

237   Adding the results of the two selected a_w intervals produced the spreading pressures at any

238   studied temperature and water activity combination.

Glass transition temperature

240   Differential scanning calorimetry was used to determine the glass transition temperature. A

241   suspension of processed foxtail millet flours and deionised water was prepared in a ratio of

242   1:3 and equilibrated for 15-18 h at ambient temperatures and were analysed using a TA

243   Instruments model Q-2000 differential scanning calorimeter, equipped with a built-in

244   software (TA Instruments, Newcastle, U.S.A.). For this, 10-12 mg of flour, equilibrated at a

245   range of water activities (0.11 – 0.85) and temperatures (10, 25 and 40 ^oC) were weighed in

246   an aluminium sample pan and hermetically sealed. A similar empty pan was used as a

247   reference for the analysis. A temperature range of -50 to 150 ^oC was used for scanning the

248   sample in the pan with a heating rate of 2 ^oC min^{-1} (Alpizar-Reyes et al. 2017). The resulting

249   thermogram gave the values of onset (T_o), peak (T_p) and conclusion temperatures (T_c) in ^oC

250   and gelatinisation enthalpies (ΔH) in kJ kg^{-1}. The final values obtained were an average of

251   three replicates for each sample, with a maximum deviation of less than 1.5%. The midpoint

252   of the baseline shift obtained using DSC was taken as the glass transition temperature (T_g).

253   The measurements were made in triplicates. Further, to deduce the plasticizing effect of water

254   on T_g, the DSC data was put in the Gordon-Taylor equation:

255   $$T_g = \frac{W_1 T_{g1} + K W_2 T_{g2}}{W_1 + K W_2}$$ (11)

256   Where, W_1 and W_2 are the mass fractions of the flours and of water, respectively, T_{g1} is the T_g

257   value of flour at zero moisture content and T_{g2} is the T_g value of water (-135 ^oC), and K is a

258   constant.

259

260

Statistical analysis

The differences amongst the samples were determined using one-way analysis of variance (ANOVA) using Minitab 17.0 software. Using the Duncan's test the differences were considered statistically significant at p-value ≤ 0.05. The degree of fitness of the model was evaluated using determination coefficient (R^2).

Results and discussion

Functional properties of the flours

The functional properties of the processed germinated foxtail millet flour (GFMF) as well as non-germinated foxtail millet flour (NGFMF) are shown in Table 1. Germination of foxtail millet increased the values of porosity, occluded air content, water and oil absorption capacity, dispersibility, swelling capacity, wettability, flowability, gelatinization enthalpy, emulsification activity and stability; while decreased the values of bulk density, insolubility index, foaming capacity and stability. Albarracín et al. (2016) reported that the water absorption and water solubility values were higher for germinated brown rice samples as compared to the control brown rice samples. Similar results were also stated by Chinma et al. (2009) for varieties of germinated tigernut flour; Devisetti et al. (2014) for millet flours and Elkhalifa and Bernhardt (2010) for germinated sorghum flour.

Moisture sorption characteristics

The effect of germination was studied for the stability of the high pressure processed foxtail millet flours.

Equilibrium moisture content- water activity

The relationship between the EMC and water activity (a_w) at a constant temperature forms the MSI. Therefore, foods with different moisture content have different water activity, thus they form their own sorption isotherm (Alpizar-Reyes et al. 2017). Fig. 2 (a, b) shows the experimental isotherms for NGFMF and GFMF at 10, 25 and 40 ºC, respectively, with which the thermodynamic functions related to moisture sorption in porridge flours were determined. Both figures depict that the EMC increased with increasing water activity ranging from 0.11 to 0.97 at a constant temperature. A constant linear increase in EMC at lower water activities ranging from 0.11 to 0.55 was observed for NGFMF and from 0.11 to 0.76 for GFMF, which

could be due to the ability of the flour to lower the vapour pressure, with the decrease in the relative humidity. While, a rapid increase in EMC at higher water activities from 0.55 to 0.97 for NGFMF (Fig. 2(a)) and an impulsive increase (Fig. 2(b)) in the EMC from 0.76 to 0.97 for GFPF could be attributed to the high sorptive capacity of hydrophilic starch in foxtail millet flours consisting of a large number of free hydroxyl sites (Pollatos et al. 2013). This impulsive increase in the case of GFMF could be because of elevated enzyme activity and breakdown of complex sugars into simple sugars during germination (Wu et al. 2013). Barreiro et al. (2003) also found similar results for malted barley flours. Therefore, it could be concluded from the results that GFMF would require improved storage conditions with relative humidity not exceeding 76% and NGFMF not exceeding 55%.

The increase in temperatures did not have a significant effect on the moisture sorption behaviour of both the flours. Though it was observed that for NGFMF, the EMC decreased with the increase in temperatures for a given water activity, showing a less hygroscopic behaviour of NGFMF at higher temperatures. This is because high temperatures increase the kinetic energy of the water molecules, thus increasing the distance between them and causing easy binding of these water molecules to the suface of the flours (Pollatos et al. 2013; Alpizar-Reyes et al. 2017). On the other hand, an opposite trend was depicted by GFMF, which could be attributed to the higher content of sugars due to germination, thus increasing the active sites for the sorption of water by proteins (Barreiro et al. 2003; Pollatos et al. 2013). In addition to this, the MSI's of both NGFMF and GFMF were of the characteristic sigmoidal shape (BET II type), which is likely found in all types of dry foods rich in starch and sugars.

Sorption models

The experimental sorption data for both the flours were fitted using GAB model, with R^2 value of more than 0.998 at all temperatures and RMSE value of less than 0.051. The model parameters were determined using non-linear regression method. Table 2 and 3 shows the model parameters for NGFMF and GFMF, respectively. MSIs of both the flours can be divided into an: (1) initial monolayer region (a_w less than 0.2), where the water molecules are strongly absorbed as critical moisture content that starts the chemical reactions in foods. It is also a measure of the availability of active sorption sites; (2) an intermediate multilayer region (a_w in the range of 0.2-0.6), that causes lipid oxidation and physical changes in foods, and (3) a final condensed water region (a_w greater than 0.6), which ascertains the microbial

11

322   growth (Labuza and Altunakar 2007). The values of monolayer moisture content (W_o) for

323   both NGFMF and GFMF decreased with the increase in temperatures from 10 to 40 ^{o}C, as

324   expected by the theory of physical sorption (Pollatos et al. 2013). The values for W_o for

325   NGFMF and GFMF ranged between 3.235 - 2.364 g g^{-1} and 2.987 – 2.063 g g^{-1}, respectively.

326   The composition and nature of the product was responsible for the difference in the values of

327   the monolayer moisture content in germinated and non-germinated flours. Thus, NGFMF

328   being a starch rich flour was found to be more hygroscopic and GFMF being a sugar rich

329   flour due to germination, was found to be less hygroscopic.

330   The constant G is related to the monolayer sorption heat which associates the chemical

331   potential difference with the superior layers of moisture in the flour structure. It has been

332   established that low temperatures assist the formation of strong adsorbent and adsorbate

333   interactions, thus causing an increase in the G values with the increase in temperature

334   (Alpizar-Reyes et al. 2017). While, this study reported a decrease in the G values on

335   increasing the temperature from 10 to 25 ^{o}C and then an increase in the G values on further

336   increasing the temperature from 25 to 40 ^{o}C, for both NGFMF and GFMF. Thus, it suggested

337   that the flour-water interactions in both NGFMF and GFMF decreased as follows: 10 ^{o}C > 40

338   ^{o}C > 25 ^{o}C. These results agreed with Pollatos et al. (2013) and Simha et al. (2016).

339   Another constant k is related to the enthalpy of water multilayer sorption indicating a measure

340   of the interactions between multilayer molecules and adsorbent. When, k values are in the

341   range of 0.24 to 1.0, GAB model best describes the sigmoid shaped isotherms (Lewicki

342   1997). For NGFMF and GFMF, the k values were in the range of 0.780 – 0.881 and 0.852 –

343   0.944, respectively. Since the values $k << 1$, so it was inferred that the flours comprised of a

344   structured state of adsorbate in the adjacent layers to the monolyer (Alpizar-Reyes et al.

345   2017).

346   *Thermodynamic properties*

347   Dried foods like the flours that have been studied here, undergo various changes during

348   storage due to the processes like crystallization, dissolution, diffusion, swelling, etc.

349   Therefore, various thermodynamic properties like integral enthalpy and entropy determines

350   the condition of maximum food stability.

351

352 Net isoteric heat of sorption

353 The degree of bound water in the flour estimates the variation in the integral enthalpy which

354 is also known as net isosteric heat of sorption (Q_{st}). It indicates the interaction of water

355 vapour with solid substrates in the flours, thus explaining the endothermic or exothermic

356 nature of the interaction (Pushpadass et al. 2014). Fig. 3 (a, b) shows the relationship between

357 Q_{st} and the moisture content at constant temperature for both NGFMF and GFMF. The

358 negative values of Q_{st} in the graph indicated the exothermic nature of sorption for both flours.

359 Strong water-substrate interactions were suggested at low moisture contents, as the water

360 binding capacity of the flours increased with the increase in the negative values of Q_{st}. The

361 values of Q_{st} ranged between -76.35 kJ mol^{-1} to -38.23 kJ mol^{-1} for NGFMF and 172.55 kJ

362 mol^{-1} to -34.02 kJ mol^{-1} for GFMF at a moisture range of 0 to 36%. At the higher moisture

363 contents, the value of Q_{st} became close to the values of heat of sorption of pure water, thus

364 indicating the excess moisture bounded to the flours or condensation in the capillaries of flour

365 particulates. The difference in the Q_{st} of both flours at low moisture contents indicated that

366 the degree of binding of water molecules was higher for GFMF as compared to the NGFMF.

367 This could be because of the availability of the higher energy polar sites on the surface in the

368 initial stages of sorption of GFMF, causing water molecules to form a monomolecular layer.

369 In addition to this, as the moisture content further increased for both the flours, the

370 availability of these sites decreased and sorption occurred at less active sites, yielding lower

371 heats of sorption (Lagoudaki and Demertzis 1994). Similar findings were observed for

372 chestnut and wheat flours (Moreira et al. 2010); Japanese durum wheat flour (Chuma et al.

373 2012); whole wheat flour (Martín- Santos et al. 2012) and Greek durum wheat semolina

374 (Pollatos et al. 2013).

375 Integral entropy

376 The integral entropy of sorption (ΔS) for NGFMF ranged between -0.404 to -0.120

377 kJ mol^{-1} K^{-1}, with a minimum value at 4% moisture content and 40 $^{\circ}$C temperature and for

378 GFMF between -0.667 to -0.383 kJ mol^{-1} K^{-1}, with a minimum value at 8% moisture content

379 and 10 $^{\circ}$C temperature. Fig. 4 (a, b) shows the integral entropy as a function of moisture

380 content at 10, 25 and 40 $^{\circ}$C for both flours. These findings were in accordance with Simha et

381 al. (2016). The minimum ΔS value was observed for GFMF as compared to NGFMF, thus

382 interpreting that GFMF is more stable than NGFMF at a temperature range of 10 to 40 $^{\circ}$C.

383 This stability is because the water molecules in the flour forms more ordered arrangement,

384   bond between adsorbate and adsorbent being the strongest. Therefore, less moisture is

385   available for spoilage reactions. The subsequent increase in the values of ΔS with the increase

386   in moisture content for both the flours, reflected the formation of multi-layers and freely held

387   molecules of water (Rizvi 1986). The increasing temperatures also had a great impact on the

388   integral entropy of both the flours. With the increase in temperature from 10 to 40 $^{\circ}$C, the

389   values of ΔS decreased for NGFMF and increased for GFMF, suggesting that NGFMF was

390   more stable at higher temperatures, while GFMF was more stable at lower temperatures. This

391   could be attributed to the composition of the flours.

392   *Enthalpy-entropy compensation theory*

393   The isokinetic theory or the enthalpy-entropy compensation theory determines the existence

394   of true compensation by comparing the difference between the harmonic temperature (T_{hm})

395   and isokinetic temperature (T_{β}) ($T_{hm} \neq T_{\beta}$). This theory helps in evaluating the sorption

396   reactions, confirming if the reactions are enthalpy driven or entropy driven. According to

397   Leffler and Grunwald (1963), if $T_{\beta} > T_{hm}$ the process is enthalpy driven, while if $T_{\beta} < T_{hm}$ the

398   process is considered to be entropy controlled. The T_{hm} values were found to be 297 K and

399   303 K at all three temperatures for NGFMF and GFMF, respectively. The results of this study

400   showed that the T_{β} values were greater than T_{hm} at all three temperatures, therefore it was

401   concluded that the sorption reactions for both NGFMF and GFMF were enthalpy-controlled

402   processes in the studied moisture content range. This further confirmed the predominance of

403   mesopores in the interactions between water-flour (Azuara and Beristain 2006). These values

404   were calculated by fitting the data in Eq. 7. Fig. 5 (a, b) depicts the enthalpy-entropy

405   compensation obtained by plotting the integral properties of both flours at constant

406   temperatures of 10, 25 and 40 $^{\circ}$C. The linear relationship between the two thermodynamic

407   properties confirmed the existence of compensation theory, which has been already justified

408   for various foods by Fontan et al. (1982).

409   *Spreading pressures*

410   The spreading pressures (π) represents the excess of free energy at the surface of the flours,

411   and provides an indication of the increase in surface tension at free sorption sites due to

412   adsorbed molecules (Fasina et al. 1999). The spreading pressure isotherms for both NGFMF

413   and GFMF were plotted against the water activity at 10, 25 and 40 $^{\circ}$C (Fig. 6 (a, b)). The

414   values of π lied in the range of 0 – 0.078 J m^{-2} for NGFMF and 0 – 0.124 J m^{-2} for GFMF,

indicating higher surface tension on the surface of GFMF at high water activities. The graph showed that the value of π increased with increasing water activity and decreased with increasing temperatures. While, at water activities above 0.76 the values of π significantly increased with increasing temperatures. Similar trend was observed for cassava flour (Ayala-Aponte 2016) and milk-foxtail millet powder (Simha et al. 2016).

Glass transition temperatures

DSC thermograms obtained for both NGFMF and GFMF at a range of water activities between 0.11 to 0.97 at 10, 25 and 40 $^{\circ}$C, gave the values of glass transition temperatures (T_g). T_g was obtained from the midpoint of the typical heat capacity change in the thermogram line over a range of temperatures (Sandoval et al. 2009). Increasing temperatures did not have any significant effect on the T_g values of both flours. Fig. 7 (a, b) shows the relationship between T_g and water activity at constant temperature. It was observed that as the water activity increased the values of T_g decreased linearly for both the flours, ranging between 82.25 to 28.67 $^{\circ}$C for NGFMF and from 51.11 to 11.83 $^{\circ}$C for GFMF at all three temperatures. The lower values of GFMF could be attributed to the conversion of starch into sugars and other compounds due to germination of foxtail millet flours. The low molecular weight of sugars and other compounds formed of germination, have been reported to cause plasticizing effect of small molecules on starchy products (Chen and Yeh 2000). While, the decrease in T_g values with increasing temperatures and water activities could be explained by the plasticizing effect of water. Increasing temperatures causes decrease in the attractive forces, thereby causing slow motion of water molecules, that gets easily adsorbed on the flour surfaces, thus decreasing the T_g values. Whereas, increasing water activities, increases the moisture content in the flours that acts as plasticizers, thus changing the glassy material into rubbery state (Alpizar-Reyes et al. 2017).

The experimental values of T_g for NGFMF and GFMF stored at different water activities and temperatures were fitted in Eq. 3.8.12 with a R^2 value of 0.991. The estimated values of T_g were found to be 124.36 $^{\circ}$C for NGFMF and 101.82 $^{\circ}$C for GFMF. This difference in the result could be due to erratic decrease in the experimental T_g values with increasing water activity, predominantly in NGFMF as compared to GFMF. Similar justification was provided for lower T_g values of dry amorphous materials in comparison to pure starch materials by Sandoval et al. (2009).

Conclusion

The germinated and non-germinated flours obtained from high pressure processed foxtail millet grains were studied for their moisture sorption characteristics to understand the interdependence between the water and the foxtail millet grain components. Thus, the moisture sorption isotherms provided information regarding the stability of these flours in any environment. Apart from this, the thermodynamic properties were also studied that gave information on the changes that took place in the flours during storage. Sorption moisture isotherms showed a sigmoidal type II shape. Experimental data for these isotherms at 10, 25 and 40 °C fitted satisfactorily to the GAB model. Sorption properties of processed germinated and non-germinated foxtail millet flour indicated that the percent of bound water decreased for NGFPF and increased for GFPF, as the temperature increased, confirming that the availability of active sites decreased due to a reduction in the total sorption ability for NGFPF and vice-versa for GFPF. This work also suggested that the moisture sorption, thermodynamic properties, spreading pressures and glass transition temperatures can be related to obtain conditions guaranteeing maximum stability for storage of the flours.

References

Abebe, W., & Ronda, F. (2015) Flowability, moisture sorption and thermal properties of tef [*Eragrostis tef* (Zucc.) Trotter] grain flours. *Journal of Cereal Science*, *63*, 14-20.

ADMI (1965). Standards for grades of dry milk including methods of analysis. *American Dry Milk Institute Bulletin*, USA.

Aguerre, R. J., Suarez, C., & Viollaz, P. E. (1986) Enthalpy- entropy compensation in sorption phenomena: Application to the prediction of the effect of temperature on food isotherms. *Journal of Food Science*. *51*(6),1547-1549.

Al-Mahasneh, M., Alkoaik, F., Khalil, A., Al-Mahasneh, A., El-Waziry, A., Fulleros, R., & Rababah, T. (2014) A generic method for determining moisture sorption isotherms of cereal grains and legumes using artificial neural networks. *Journal of Food Process Engineering*, *37*, 308-316.

475　Albarracín, M., Talens, P., Martínez-Navarrete, N., González, R. J., & Drago, S. R. (2016)
476　　　　Physicochemical properties and structural characteristics of whole grain *Oryza*
477　　　　*sativa* L. with different treatments. *Food Science and Technology*
478　　　　*International*, *22*(4), 333-342.

479　Alpizar-Reyes, E., Carrillo-Navas, H., Romero-Romero, R., Varela-Guerrero, V., Alvarez-
480　　　　Ramírez, J., & Pérez-Alonso, C. (2017) Thermodynamic sorption properties and
481　　　　glass transition temperature of tamarind seed mucilage (*Tamarindus indica* L.).
482　　　　*Food and Bioproducts Processing. 101*, 166-176.

483　Arslan, N., & Togrul, H. (2006) The fitting of various models to water sorption isotherms of
484　　　　tea stored in a chamber under controlled temperature and humidity. *Journal of*
485　　　　*Stored Products Research*, *42*(2), 112- 135.

486　Ayala-Aponte, A. A. (2016) Thermodynamic properties of moisture sorption in cassava
487　　　　flour. *Dyna*, *83*(197), 138-144.

488　Azuara, E., & Beristain, C. I. (2006) Enthalpic and entropic mechanisms related to water
489　　　　sorption of yogurt. *Drying Technology*, *24*(11), 1501-1507.

490　Barreiro, J. A., Fernández, S., & Sandoval, A. J. (2003) Water sorption characteristics of six
491　　　　row barley malt (*Hordeum vulgare*). *LWT-Food Science and Technology*, *36*(1),
492　　　　37-42.

493　Bell, L. N., & Labuza, T. P. (2000) Moisture Sorption: Practical Aspects of Isotherm
494　　　　Measurement and Use. St. Paul, Minnesota, USA: *American Association of Cereal*
495　　　　*Chemists*.

496　Brett, B., Figueroa, M., Sandoval, A. J., Barreiro, J. A., & Müller, A. J. (2009) Moisture
497　　　　sorption characteristics of starchy products: oat flour and rice flour. *Food*
498　　　　*Biophysics*, *4*(3), 151-157.

499　Chen, C. M., & Yeh, A. I. (2000) Expansion of rice pellets: Examination of glass transition
500　　　　and expansion temperature. *Journal of Cereal Science*, *32*(2), 137–145.

501 Chinma, C. E., Adewuyi, O., & Abu, J. O. (2009) Effect of germination on the chemical,
502   functional and pasting properties of flour from brown and yellow varieties of
503   tigernut (*Cyperus esculentus*). *Food Research International*, *42*(8), 1004-1009.

504 Chuma, A., Ogawa, T., Kobayashi, T., & Adachi, S. (2012) Moisture sorption isotherm of
505   durum wheat flour. *Food Science and Technology Research*, *18*(5), 617-622.

506 Devisetti, R., Yadahally, S. N., & Bhattacharya, S. (2014) Nutrients and antinutrients in
507   foxtail   and   proso   millet   milled   fractions: Evaluation   of   their   flour
508   functionality. *LWT-Food Science and Technology*, *59*(2), 889-895.

509 Elkhalifa, A. E. O., & Bernhardt, R. (2010) Influence of grain germination on functional
510   properties of sorghum flour. *Food Chemistry*, *121*(2), 387-392.

511 Erbaş, M., Aykin, E., Arslan, S., & Durak, A. N. (2016) Adsorption behaviour of bulgur.
512   *Food Chemistry*, *195*, 87-90.

513 Estrada-Girón, Y., Swanson, B. G., & Barbosa-Cánovas, G. V. (2005) Advances in the use of
514   high hydrostatic pressure for processing cereal grains and legumes. *Trends in Food
515   Science and Technology*, *16*, 194-203.

516 Fasina, O. O., Ajibola, O. O., & Tyler, R. T. (1999) Thermodynamics of moisture sorption in
517   winged bean seed and gari. *Journal of Food Process Engineering*, *22*(6), 405-418.

518 Fasina, O., Sokhansanj, S., & Tyler, R. (1997) Thermodynamics of moisture sorption in
519   alfalfa pellets. *Drying Technology*, *15*(5), 1553-1570.

520 Fontan, C. F., Chirife, J., Sancho, E., & Iglesias, H. A. (1982) Analysis of a model for water
521   sorption phenomena in foods. *Journal of Food Science*, *47*(5), 1590-1594.

522 Greenspan, L. (1977) Humidity fixed points of binary saturated aqueous solutions. *Journal of
523   Research of the National Bureau of Standards*, *81*(1), 89-96.

524 Iglesias, H. A., Chirife, J., & Viollaz, P. (1976) Thermodynamics of water vapour sorption by
525   sugar beet root. *Journal of Food Technology*, *11*(1), 91- 101.

526   Ikhu- Omoregbe, D. I. O., & Chen, X. D. (2005) Use of sorption isotherms for the estimation
527   of shelf life of two Zimbabwean flours. *Developments in Chemical Engineering*
528   *and Mineral Processing*, *13*(1- 2), 79-90.

529   Jha, A., Patel, A. A., & Singh, R. R. B. (2002) Physico-chemical properties of instant *kheer*
530   mix. *Le Lait*, *82*(4), 501-513.

531   Katz, E. E., & Labuza, T. P. (1981) Effect of water activity on the sensory crispness and
532   mechanical deformation of snack food products. *Journal of Food Science*, *46*(2),
533   403-409.

534   Kaya, S., & Kahyaoglu, T. (2005) Thermodynamic properties and sorption equilibrium of
535   pestil (grape leather). *Journal of Food Engineering*, *71*(2), 200-207.

536   Krug, R. R., Hunter, W. G., & Grieger, R. A. (1976) Enthalpy-entropy compensation. 2.
537   Separation of the chemical from the statistical effect. *The Journal of Physical*
538   *Chemistry*, *80*(21), 2341-2351.

539   Labuza, T. P., Kaanane, A., & Chen, J. Y. (1985) Effect of temperature on the moisture
540   sorption isotherms and water activity shift of two dehydrated foods. *Journal of*
541   *Food Science*, *50*(2), 385-392.

542   Labuza, T. P., & Altunakar, B. (2007) Water activity prediction and moisture sorption
543   isotherms. *Water activity in foods: fundamentals and applications*, John Wiley &
544   Sons, *1*, 109-131.

545   Lagoudaki, M., & Demertzis, P. G. (1994) Equilibrium moisture characteristics of dehydrated
546   food constituents as studied by a modified inverse gas chromatographic
547   method. *Journal of the Science of Food and Agriculture*, *65*(1), 101-109.

548   Lagoudaki, M., Demertzis, P. G., & Kontominas, M. G. (1993) Moisture adsorption
549   behaviour of pasta products. *LWT-Food Science and Technology*, *26*(6), 512-516.

550   Lakon, G. (1949) The topographical tetrazolium method for determining the germinating
551   capacity of seeds. *Plant Physiology*, *24*(3), 389.

552 Lang, K. W., McCune, T. D., & Steinberg, M. P. (1981) A proximity equilibration cell for
553   rapid determination of sorption isotherms. *Journal of Food Science*, *46*(3), 936-
554   938.

555 Lasekan, O. O., & Lasekan, W. O. (2000) Moisture sorption and the degree of starch polymer
556   degradation on flours of popped and malted sorghum (*Sorghum bicolor*). *Journal
557   of cereal science*, *31*(1), 55-61.

558 Leffler, J. E., & Grunwald, E. (1963) *Rates and equilibria of organic reactions: as treated by
559   statistical, thermodynamic, and extrathermodynamic methods*. John Wiley & Sons,
560   Dover Publications, New York.

561 Lewicki, P. P. (1997) The applicability of the GAB model to food water sorption
562   isotherms. *International journal of food science & technology*, *32*(6), 553-557.

563 Martín- Santos, J., Vioque, M., & Gómez, R. (2012) Thermodynamic properties of moisture
564   adsorption of whole wheat flour. Calculation of net isosteric heat. *International
565   Journal of Food Science & Technology*, *47*(7), 1487-1495.

566 McMinn, W. A. M., & Magee, T. R. A. (2003) Thermodynamic properties of moisture
567   sorption of potato. *Journal of Food Engineering*, *60*(2), 157-165.

568 Moreira, R., Chenlo, F., Torres, M. D., & Prieto, D. M. (2010) Water adsorption and
569   desorption isotherms of chestnut and wheat flours. *Industrial crops and
570   products*, *32*(3), 252-257.

571 Muers, M. M., & House, T. U. (1962) A simple method for comparing wettability of instant
572   spray dried separated milk powder. In *Copenhagen, Denmark: XVI International
573   Dairy Congress*, *8*, 299.

574 Ondier, G. O., Siebenmorgen, T. J., & Mauromoustakos, A. (2012) Equilibrium moisture
575   contents of pureline, hybrid, and parboiled rice kernel fractions. *Applied
576   Engineering in Agriculture*, *28*(2), 237.

577 Pérez-Alonso, C., Beristain, C. I., Lobato-Calleros, C., Rodríguez-Huezo, M. E., & Vernon-
578   Carter, E. J. (2006) Thermodynamic analysis of the sorption isotherms of pure and
579   blended carbohydrate polymers. *Journal of Food Engineering*, *77*(4), 753-760.

580   Pollatos, E. P., Riganakos, K. A., & Demertzis, P. G. (2013) Moisture sorption characteristics
581   of Greek durum wheat semolina. *Starch‐ Stärke*, *65*(11-12), 1051-1060.

582   Pushpadass, H. A., Emerald, F., Chaturvedi, B., & Rao, K. J. (2014) Moisture sorption
583   behavior and thermodynamic properties of *gulabjamun* mix. *Journal of Food
584   Processing and Preservation*, *38*(6), 2192-2200.

585   Rizvi, S. S. H. (1986) Thermodynamic properties of foods in dehydration. In: Rao MA, Rizvi
586   SSH, Datta AK (eds), *Engineering properties of food*, 3rd ed. CRC Press, Boca
587   Raton.

588   Rizvi, S. S. H., & Benado, A. L. (1983) Thermodynamic analysis of drying foods. *Drying
589   Technology*, *2*(4), 471-502.

590   Sandoval, A. J., Nuñez, M., Müller, A. J., Della Valle, G., & Lourdin, D. (2009) Glass
591   transition temperatures of a ready to eat breakfast cereal formulation and its main
592   components determined by DSC and DMTA. *Carbohydrate Polymers*, *76*(4), 528-
593   534.

594   Sharma, S., Saxena, D.C., & Riar, C.S. (2015) Antioxidant activity, total phenolics,
595   flavonoids and antinutritional characteristics of germinated foxtail millet (*Setaria
596   italica*). *Cogent Food & Agriculture*, *1*(1), 1081728.

597   Sharma, N., & Niranjan, K. (2017) Foxtail millet: properties, processing, health benefits and
598   uses. *Food Reviews International*, DOI: 10.1080/87559129.2017.1290103.

599   Simha, H. V., Pushpadass, H. A., Franklin, M. E. E., Kumar, P. A., & Manimala, K. (2016)
600   Soft computing modelling of moisture sorption isotherms of milk-foxtail millet
601   powder and determination of thermodynamic properties. *Journal of food science
602   and technology*, *53*(6), 2705-2714.

603   Sjollema, A. (1963) Some investigations on the free-flowing properties and porosity of milk
604   powders. *Netherlands Milk and Dairy Journal*, *17*(3), 245-259.

605   Sodipo, M. A., & Fashakin, J. B. (2011) Physicochemical properties of a complementary diet
606   prepared from germinated maize, cowpea and pigeon
607   pea. *Journal of Food, Agriculture and Environment*, *9*(3-4), 23-25.

608 VICH Steering Committee (2002) Testing of residual formaldehyde. *VICH International*
609 *Cooperation on Harmonization of Technical Registration of Veterinary Medical*
610 *Products*, 4-6.

611 Wu, F., Chen, H., Yang, N., Wang, J., Duan, X., Jin, Z., & Xu, X. (2013) Effect of
612 germination time on physicochemical properties of brown rice flour and starch
613 from different rice cultivars. *Journal of Cereal Science*, *58*(2), 263-271.

614 Yu, Y., Ge, L., Ramaswamy, H. S., Wang, C., Zhan, Y., & Zhu, S. (2016) Effect of high-
615 pressure processing on moisture sorption properties of brown rice. *Drying*
616 *Technology*, *34*(7), 783-792.

617 Zhang, Q., Ge, L., Ramaswamy, H. S., Zhu, S., Yu, L., & Yu, Y. (2017) Modeling
618 Equilibrium Moisture Content of Brown Rice as Affected by High-Pressure
619 Processing. *Transactions of the ASABE*, *60*(2), 551-559.

620 Zhang, L., Li, J., Han, F., Ding, Z., & Fan, L. (2017) Effects of different processing methods
621 on the antioxidant activity of 6 cultivars of foxtail millet. *Journal of Food Quality*,
622 DOI: 10.1155/2017/8372854.

623

624

625

626

627

628

629

630

631

632

633

634

635

636

637

TABLES

Table 1   Functional properties of processed foxtail millet flours

Property	GFMF	NGFMF
Bulk density (g l^{-1})	592 ± 12.2^b	732 ± 10.4^a
Porosity (% volume)	67.8 ± 0.5^a	53.4 ± 0.6^b
Occluded air content (ml $100ml^{-1}$)	105.3 ± 2.0^a	94.6 ± 1.8^b
Water absorption capacity (g $100g^{-1}$)	157.4 ± 1.8^a	148.2 ± 2.3^b
Oil absorption capacity (g $100g^{-1}$)	98.0 ± 0.5^a	80.4 ± 1.1^b
Dispersibility (%)	82.2 ± 0.5^a	75.4 ± 0.3^b
Insolubility index (ml)	3.1 ± 0.2^b	4.7 ± 0.1^a
Swelling capacity (ml g^{-1})	5.2 ± 0.2^a	4.0 ± 0.3^b
Wettability (s)	58.0 ± 1.0^a	52.0 ± 1.0^b
Flowability (θ)	70.1 ± 0.4^a	62.3 ± 0.9^b
Emulsion activity (%)	64.5 ± 0.1^a	48.2 ± 0.0^b
Emulsion stability (%)	82.4 ± 0.2^a	66.5 ± 0.1^b
Foaming capacity (%)	5.2 ± 0.4^b	8.8 ± 0.5^a
Foaming stability (%)	57.8 ± 0.7^b	78.8 ± 0.9^a
Gelatinization properties:		
1. Onset temperature (°C)	70.05 ± 0.92^a	70.05 ± 1.03^a
2. Peak temperature (°C)	73.16 ± 1.11^a	73.01 ± 1.13^a
3. Conclusion temperature (°C)	77.25 ± 0.88^a	77.13 ± 0.98^a
4. Gelatinization enthalpy (J/g)	2.306 ± 0.110^a	1.563 ± 0.099^b

Values are mean of three replications (n=3) and expressed as mean ± standard deviation.
Means with different superscript within the same row are significantly different at $p \leq 0.05$.

23

647

Table 2   Estimated parameters of GAB sorption model for NGFMF

T (°C)	W_o (%)	G	k	R^2
10	3.235±0.100[a]	43.171±0.150[a]	0.780±0.020[a]	0.99
25	2.662±0.150[b]	28.260±0.200[b]	0.820±0.020[a]	0.99
40	2.364±0.090[b]	32.720±0.190[c]	0.881±0.025[a]	0.99

649   Values are mean of three replications (n=3) and expressed as mean ± standard deviation.

650

Table 3   Estimated parameters of GAB sorption model for GFMF

T (°C)	W_o (%)	G	k	R^2
10	2.987±0.090[a]	42.701±0.220[a]	0.852±0.025[a]	0.99
25	2.476±0.095[a]	28.912±0.150[b]	0.896±0.030[a]	0.98
40	2.063±0.090[a]	33.661±0.150[c]	0.944±0.010[a]	0.99

652   Values are mean of three replications (n=3) and expressed as mean ± standard deviation.

653

654

655

656

657

658

659

660

661

662

663

664

665

666

667 **FIGURES**

668
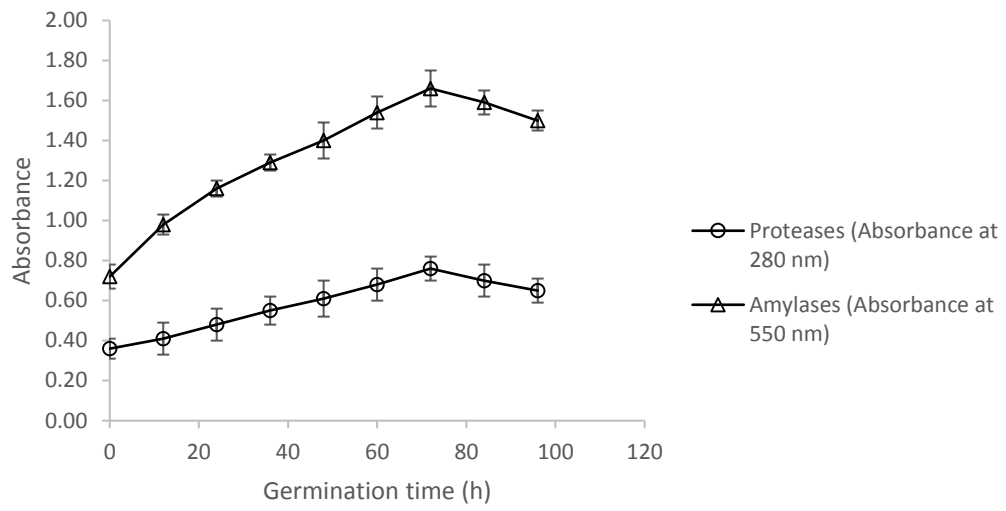
Fig. 1   Protease and amylase activity variation during the germination of foxtail millet
670   grains (Temperature= 25±2 °C; RH=80%)

671

672

673

674

675

676
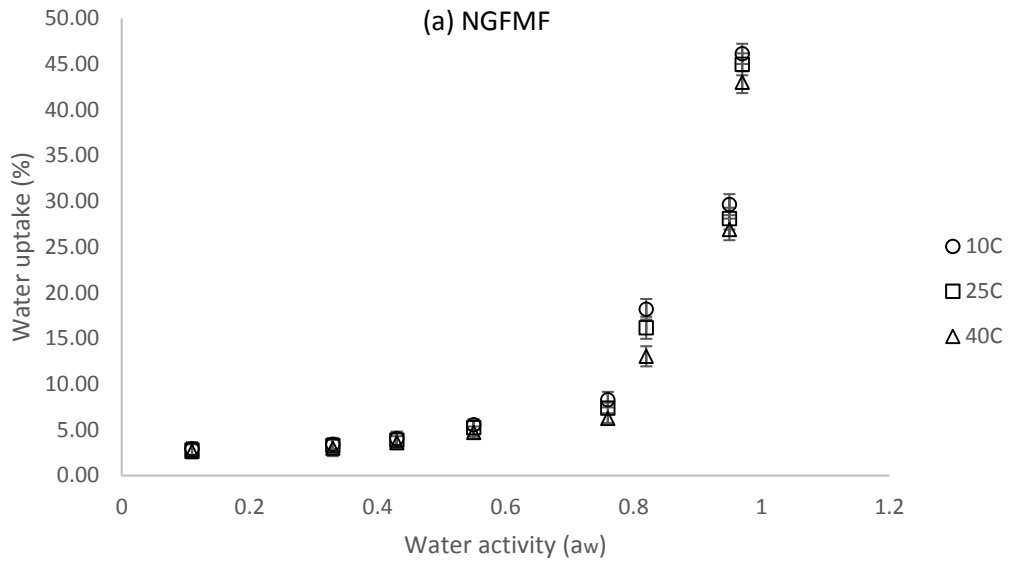
677

678
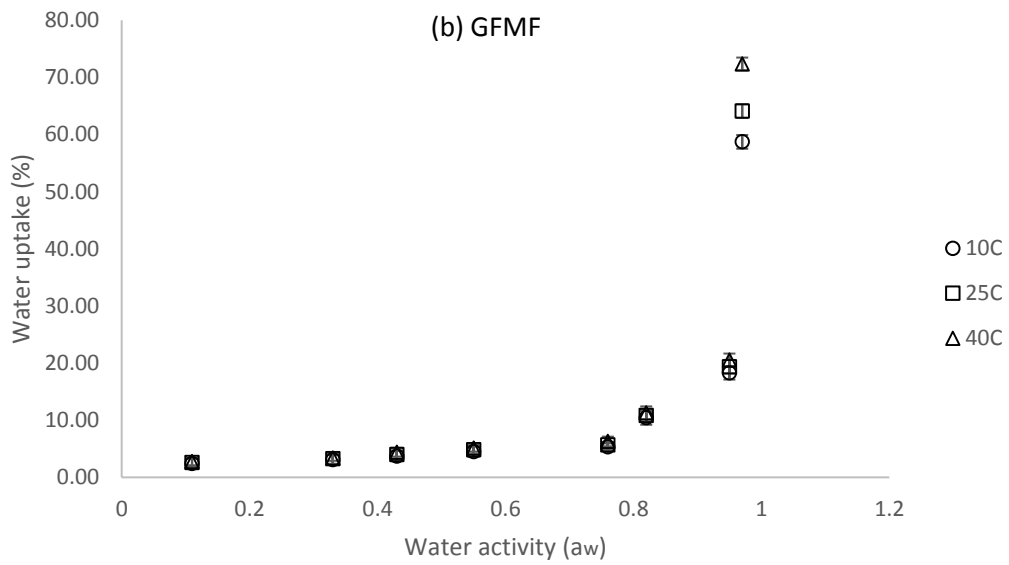
679

680 **Fig. 2** Moisture sorption isotherms for (a) NGFMF and (b) GFMF at 10, 25 and 40 ºC

681 obtained by static gravimetric method

682
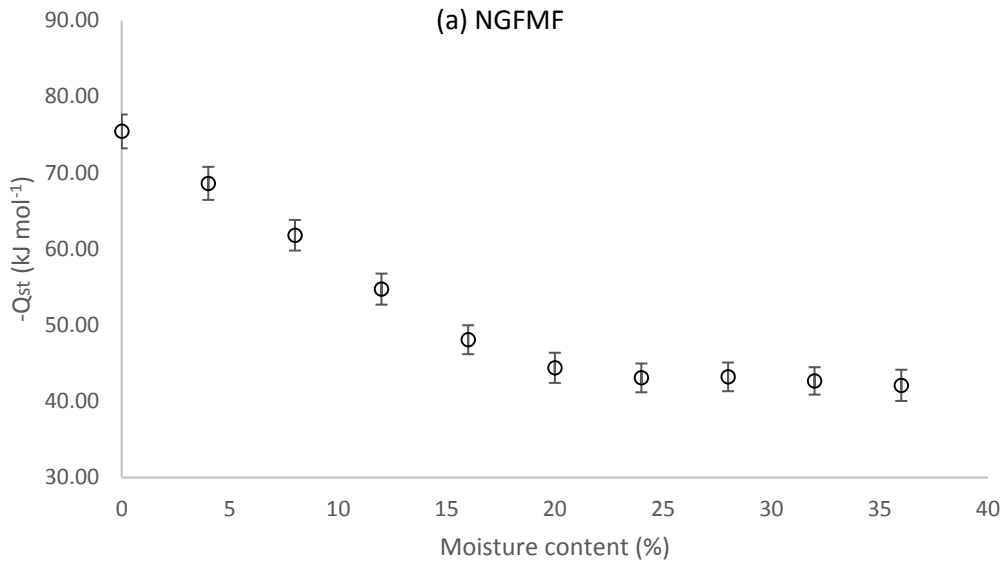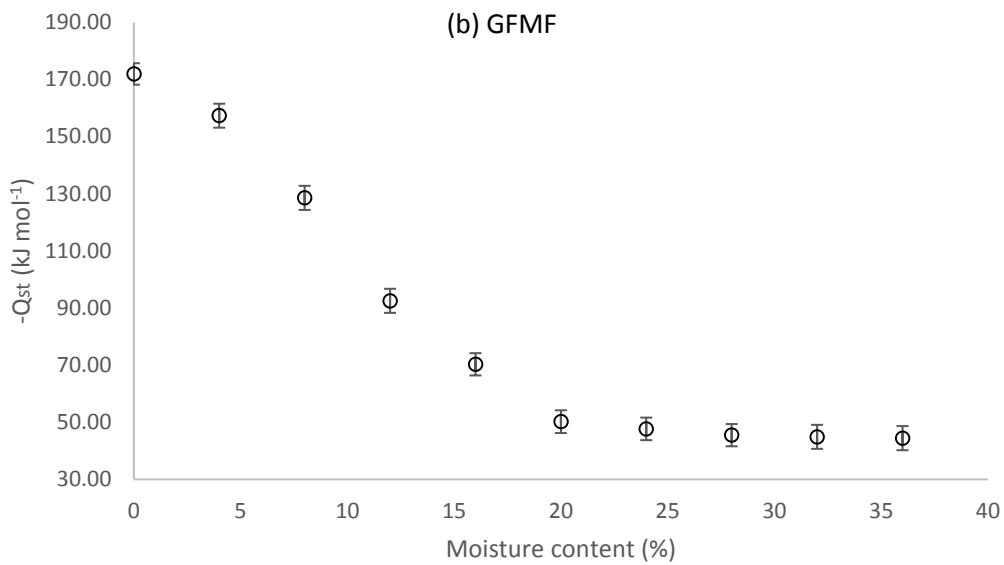
(a) NGFMF

(b) GFMF

Fig. 3   Net isosteric heat of sorption (Q_{st}) as a function of moisture content for (a) NGFMF and (b) GFMF. The isoteric heat of sorption at any temperature can be obtained by adding the latent heat at that temperature to the Qst values.

686
687
688

689
690
691
692
693

27

694

695
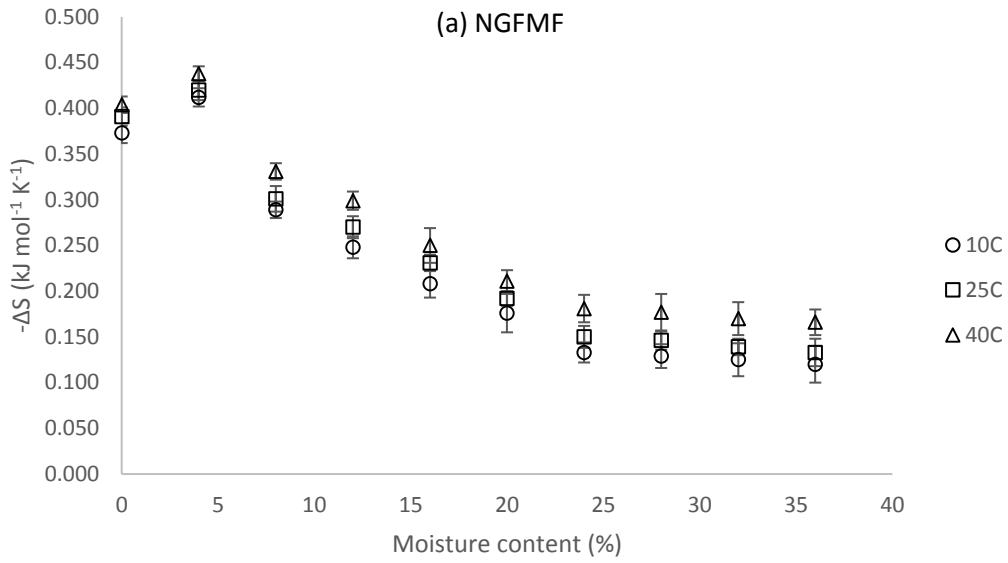
696

697
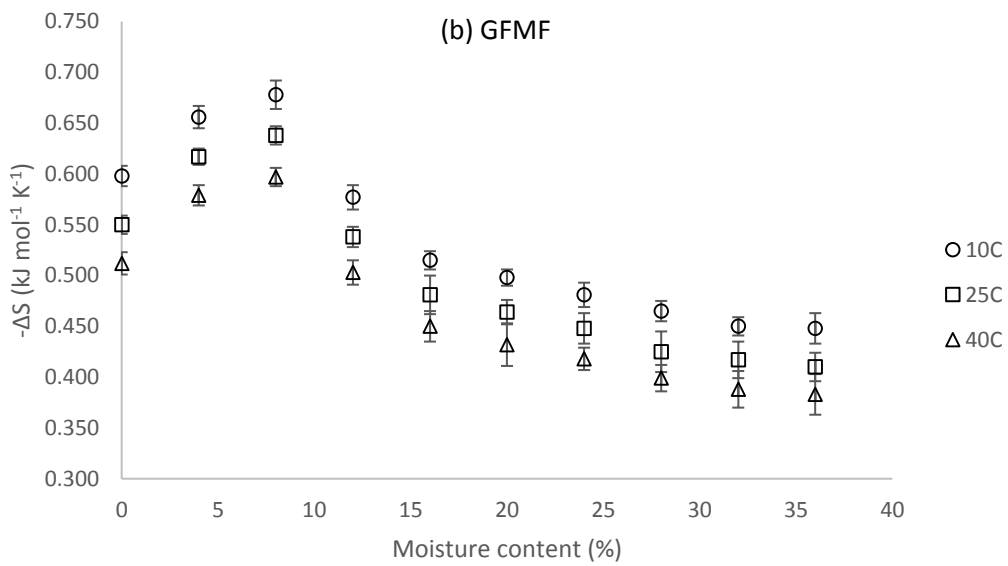
698

699 **Fig. 4**   Integral entropy (ΔS) as a function of moisture content of (a) NGFMF and (b)

700   GFMF

701

702
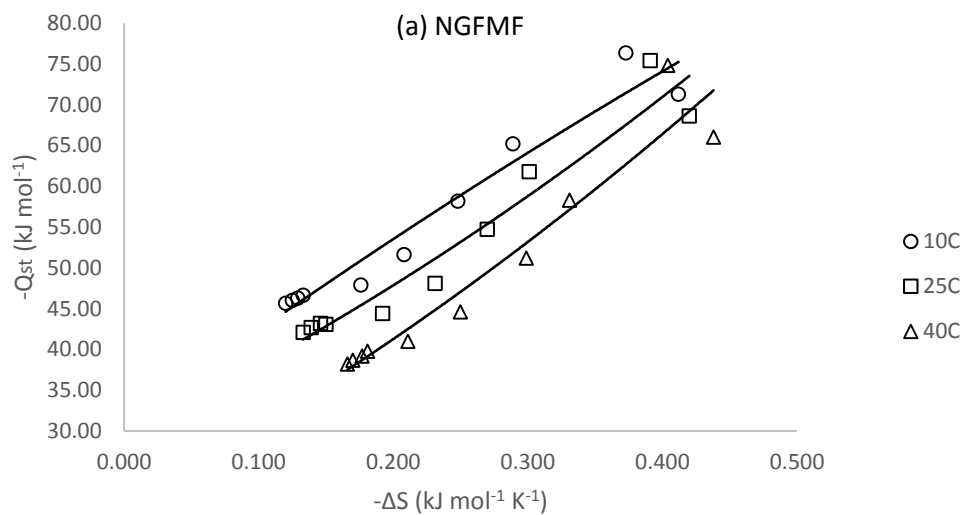
703
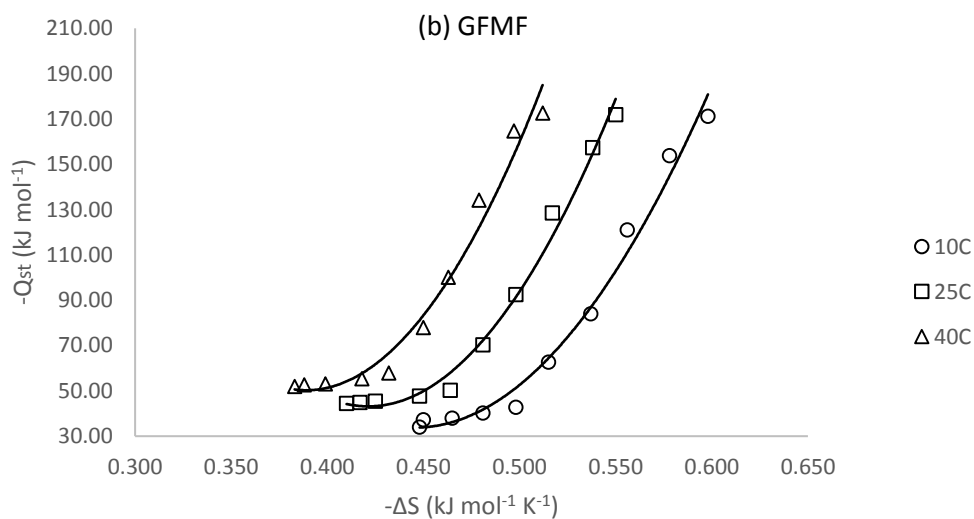
704

705 **Fig. 5**   Integral enthalpy-integral entropy compensation for (a) NGFMF and (b) GFMF
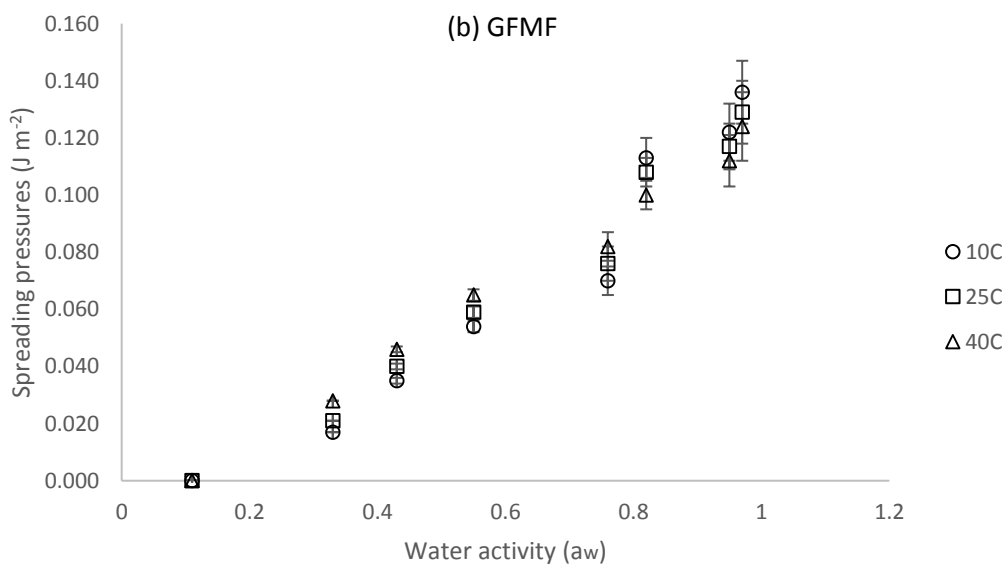
706

707

708

709

710
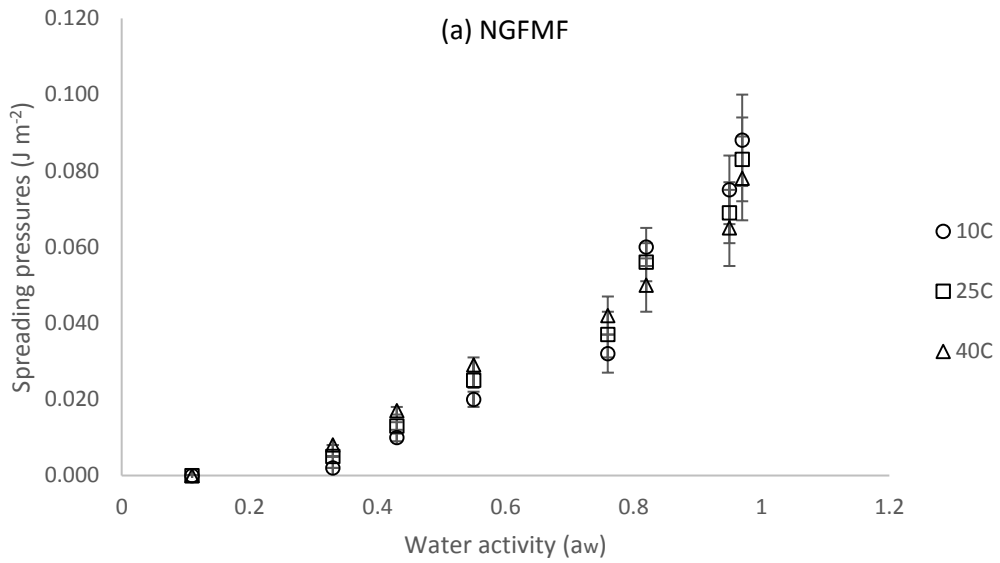
711

712

713

714 **Fig. 6** Spreading pressure isotherms as a function of water activity of (a) NGFMF and
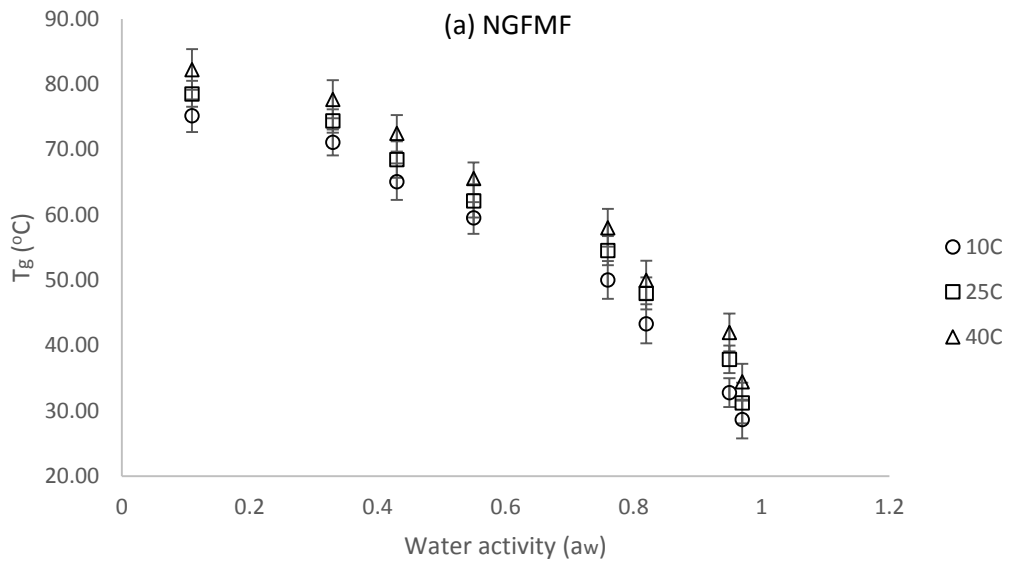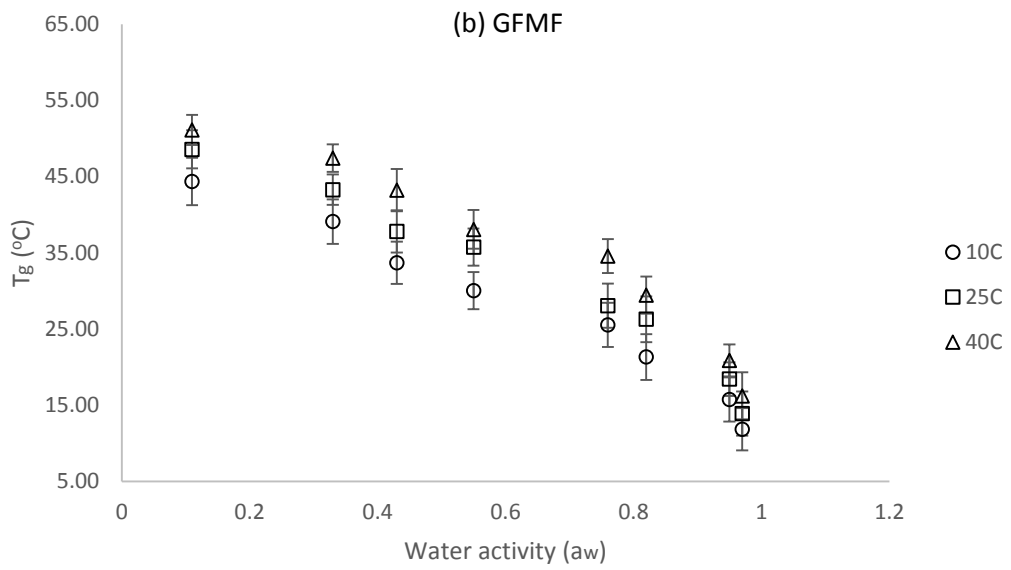715 (b) GFMF

716

717

718

719

720

721

722

Fig. 7   Effect of water activity on glass transition temperatures of (a) NGFMF and (b)
         GFMF

725

726